Analysis of the isotope effect of high-T_c ceramic $YBa_{2-x}La_xCu_3O_7$ using the excitonic-enhancement model

K. W. Wong,* P. C. W. Fung, H. Y. Yeung, and W. Y. Kwok
Department of Physics, University of Hong Kong, Hong Kong
(Received 19 August 1991; revised manuscript received 13 November 1991)

The excitonic-enhancement model (EEM) is based on the simultaneous excitonic and "generalized" Cooper-pair condensation of a charge-unbalanced system that is described by a two-band model consisting of a valence and a conduction band separated by a band gap G. A detailed numerical analysis of the consequences of the EEM with respect to shift of T_c due to the oxygen isotope effect on the La-doped Y-Ba-Cu-O system is carried out. The results are found to be in excellent agreement with the recent experimental data of Bornemann and Morris, covering a T_c range of 38.3–92.3 K.

I. INTRODUCTION

One of the intriguing experimental properties of high-T_c superconductors is the exceptionally small but finite isotope effect reported in systems with T_c's above 77 K. For such T_c values, the transition temperature is quite insensitive to the isotopic mass M of the constituent atoms: If one expresses the T_c-M relation in the usual manner

$$T_c \propto M^{-\alpha_0}, \tag{1}$$

then α_0 is found experimentally to lie within the range 0.0–0.025 for ceramic superconductors having $T_c > 77$ K. In fact, many isotope-effect studies involving ^{18}O substitution experiments were performed on the ceramic $YBa_2Cu_3O_{7-\delta}$. These studies tend to agree on the result that $\alpha_0 = 0.02$.[1–5] The isotope mass power α of Cu for $YBa_2Cu_3O_{7-\delta}$ was found by Bonrne *et al.*[6] and Lin *et al.*[7] to be even less. In fact limits have been set in Ref. 6 on the Ba-isotope mass power $\alpha_0 = 0.0 \pm 0.1$ for $YBa_2Cu_3O_{7-\delta}$. However, the oxygen-isotope mass power in $La_{1.85}Sr_{0.15}CuO_4$ was determined to be much higher, being $\alpha_0 = 0.15$.[8–10] It therefore appears that the existence of La might also introduce a larger oxygen isotope effect in the Y-Ba-Cu-O system. Indeed, it has been found recently that the oxygen-isotope T_c shift of the specimen $YBa_{2-x}La_xCu_3O_7$ is much enhanced at high La doping and low critical temperatures. At $T_c = 38.3$ K, α_0 was reported as large as 0.38 and α_0 was found to decrease for the six samples with lesser doping. Their results seem to suggest that the conventional electron-phonon coupling plays a dominant role in cuprate ceramic superconductors, since a strong suppression of the isotope effect is related to the increase in T_c values. A full understanding of the isotope effect on T_c could therefore reveal useful information on the high-T_c mechanism.

In this paper we shall examine the isotope effect from the exitonic-enhancement model (EEM) theory[11,12] suggested earlier and compare its consequences with the recent new experimental data.[13] Our analysis based on EEM theory indicates excellent agreement with the experimental work.

In Sec. II we review briefly the essence of EEM, listing the transformations involved and derive the analytic forms of the charge-excitonic gap function Δ_{ex} and the Bardeen-Cooper-Schriefer (BCS) gap function Δ_{BCS} for the two-band model. We should note in particular the Δ_{BCS} function within the EEM is a "generalized one" in the sense that Δ_{BCS} now depends not only on the Debye frequency ω_D, the coupling strength J, the Fermi energy $\bar{\mu}$ (as measured from the middle of the band gap), but also on the effective band gap G^* between the valence and conduction bands (which include electron-phonon interaction corrections) plus the charge-excitonic gap Δ_{ex}. In other words, Δ_{ex} and Δ_{BCS} are linked together and the condensed Cooper pairs in EEM theory are holes dressed by electrons.

We carry out a detailed numerical analysis in Sec. III using the recent experimental data of Bornemann and Morris[13] and the thermodynamic equation resulting from the EEM. It is remarkable to note that though we have obtained the explicit forms of $\bar{\mu}, \Delta_{BCS}, \Delta_{ex}$ through curve fitting, these explicit expressions contain the crucial physical ideas behind the mechanism. We conclude this paper in Sec. IV and discuss some possible future experimental works that might aid in testing further the EEM as the high-T_c superconducting mechanism.

II. THE EXCITONIC-ENHANCEMENT MODEL

The excitonic enhancement model (EEM) put forward by Wong *et al.*[11,12] is based on the simultaneous excitonic and superconductivity condensation of a charge-unbalanced system, which is described by a two-energy-band model, specified by bands, ε_a and ε_b [cf. Eqs. (3a) and (3b) of Ref. 11].

One of the important results of EEM is that it successfully relates the excitonic gap function $\Delta_{ex}(\mathbf{p})$, at momentum $\mathbf{p}$, with the two-band energy spectrum and the BCS phonon interaction as[11]

$$\Delta_{ex}(\mathbf{p}) = \frac{1}{2(2\pi)^3} \int d^3q \, V_c(\mathbf{q}) \left\{ \frac{\Delta_{ex}(\mathbf{p}+\mathbf{q})}{[\xi^2_{\mathbf{p}+\mathbf{q}} + \Delta^2_{ex}(\mathbf{p}+\mathbf{q})]^{1/2}} \right\}, \tag{2}$$

where

$$\xi_{\mathbf{k}}=\frac{\varepsilon_b-\varepsilon_a}{2}+\Lambda_k \tag{3}$$

and

$$\Lambda_k=\tfrac{1}{2}\sum_{\mathbf{q}}J(\mathbf{k}-\mathbf{q})\{U_{\mathbf{k}}^2-V_{\mathbf{k}}^2\}\ , \tag{4}$$

in which J is the phonon interaction, $U_{\mathbf{k}}$ and $V_{\mathbf{k}}$ are the coefficients of canonical transformation from particles to quasiparticles, and V_c measures the interband Coulomb interaction.

After rearrangement and expansion, Eq. (2) can be written as

$$\left\{\frac{\hbar^2p^2}{2m_\alpha}+\Lambda_p-G-\frac{\Delta_{\rm ex}^2}{2(G-\Lambda_p)}\right\}\psi_{\rm ex}(\mathbf{p})=\frac{1}{2(2\pi)^3}\int d^3q\ V_c(\mathbf{q})\psi_{\rm ex}(\mathbf{p}+\mathbf{q})\ , \tag{5}$$

where m_α is the quasihole mass and G is the energy gap between the valence (VB) and conduction (CB) bands.

Equation (5) is similar to the equation for a hydrogenic system. We therefore identify the Bohr energies, E_n, as

$$E_n=\frac{\Delta_{\rm ex}^2}{2(G-\Lambda_p)}-\Lambda_p+G\ . \tag{6}$$

Upon performing a second canonical transformation from quasiparticle to quasiparticle pairs,[11] one obtains the gap equation relating the BCS gap and the quasiparticle energy E as follows:

$$\Delta_{\rm BCS}=\int_{-\hbar\omega_D}^{\hbar\omega_D}N_F\bar{J}(E)\Gamma\frac{\Delta_{\rm BCS}}{2(E^2+\Delta_{\rm BCS}^2)^{1/2}}dE\ . \tag{7}$$

The quasiparticle energy spectrum E, as a function of momentum k, can be shown to be given by[11]

$$E_k=-\bar{\mu}+(\xi_k^2+\Delta_{\rm ex}^2)^{1/2}\ . \tag{8}$$

In Eq. (7), N_F is the Fermi density of the quasiparticles, $\bar{J}$ is the effective phonon interaction [see Eqs. (2.10) and (2.12) of Ref. 11 for definition] and the domain of integration had been changed from quasiparticle momentum space to the quasiparticle energy E [cf. Eq. (2.32) of Ref. 11]. In this transformation a phase factor $\Gamma=\Gamma(\Delta_{\rm ex},\bar{\mu},G^*)$ occurs expressible as

$$\Gamma=\left[\frac{1}{\sqrt{1-X}}-\frac{G^*}{2\bar{\mu}(1-X)}\right]^{1/2}\ , \tag{9}$$

where $X=(\Delta_{\rm ex}/\bar{\mu})^2$, $G^*=G-\Lambda_p$, and $\bar{\mu}$ is the Fermi energy.

Analogous to BCS theory, the solution to Eq. (7) is

$$\Delta_{\rm BCS}=2\hbar\omega_D\exp\left[\frac{-1}{\bar{J}(k_F)N_F\Gamma}\right]\ , \tag{10}$$

which is now coupled to the excitonic gap through the phase factor Γ.

Another important result of Ref. 11 is that the final quantum-fluid excitation spectrum is

$$E_{\rm ex}(k)=(E_k^2+\Delta_{\rm BCS}^2)^{1/2}=\{(\xi_{\mathbf{k}}-\bar{\mu})^2+\Delta_T^2\}^{1/2}\ , \tag{11}$$

where the last form emphasizes the resemblance to the case of BCS theory, with $\Delta_{\rm BCS}$ replaced by the total gap Δ_T defined as,[11]

$$\Delta_T^2=\Delta_{\rm BCS}^2+\bar{\Delta}_{\rm ex}^2\ , \tag{12}$$

in which $\bar{\Delta}_{\rm ex}$ is related to $\Delta_{\rm ex}$ and quasiparticle energy ξ_k [see Eq. (2.39) of Ref. 11 for definition of $\bar{\Delta}_{\rm ex}$].

III. THE EEM THERMODYNAMIC EQUATION AND ANALYSIS OF THE ISOTOPE EFFECT

In the review and discussion presented in the preceding section, the concept of temperature has not yet been introduced. If we are to simply extend from the BCS gap $T=0$ equation to the same gap equation for finite temperature,

$$\Delta_{\rm BCS}=J\int_{-\hbar\omega_D}^{\hbar\omega_D}N_F^*\frac{\Delta_{\rm BCS}}{2E_{\rm ex}}\tanh\left[\frac{\beta E_{\rm ex}}{2}\right]dE\ , \tag{13}$$

where $E_{\rm ex}=(E^2+\Delta_{\rm BCS}^2)^{1/2}(E=E_k)$, $\beta=1/kT$, $N_F^*=N_F\Gamma$, and J is the phonon mediated interaction coupling. Since the energy E depends only on $\bar{\Delta}_{\rm ex}$, the diagonal long-range-ordering excitonic amplitude, this equation is not symmetric in $\Delta_{\rm BCS}$ and $\bar{\Delta}_{\rm ex}$. In the process of evaluating T_c we need to consider the situation where we break both $\Delta_{\rm BCS}$ and $\bar{\Delta}_{\rm ex}$. However, Eq. (13) does not have a unique solution when we interchange the order of limits $\Delta_{\rm BCS}\to 0$ and $\bar{\Delta}_{\rm ex}\to 0$ in our evaluation of T_c. The EEM theory requires the simultaneous breaking of $\Delta_{\rm BCS}$ and $\bar{\Delta}_{\rm ex}$, thus the thermodynamic equation governing T_c must be given in terms of the thermal averaging of the total gap Δ_T. With these requirements, we set

$$\Delta_T=J\int_{-u}^{u}N_F^*\frac{\Delta_T}{2E_{\rm ex}}\tanh\left[\frac{\beta E_{\rm ex}}{2}\right]d\xi\ , \tag{14}$$

where $\xi=\xi_k-\varepsilon_F$ [$\neq E_k$ as given by Eq. (8) and $\varepsilon_F=\bar{\mu}$]. On the other hand, when the conventional Cooper pair ceases to exist, i.e., when $\hbar\omega_D=0$, our thermodynamic equation must also describe the situation $\Delta_T\to\bar{\Delta}_{\rm ex}$. In order that Eq. (14) can reduce to $\bar{\Delta}_T\to\bar{\Delta}_{\rm ex}$ when $\hbar\omega_D=0$,

$$\bar{\Delta}_{\rm ex}=\lim_{\hbar\omega_D\to 0}J\int_{-u}^{u}N_F^*\frac{\bar{\Delta}_{\rm ex}}{2E_{\rm ex}}\tanh\left[\frac{\beta E_{\rm ex}}{2}\right]d\xi\ , \tag{15}$$

and that at $T=0$, Δ_T must be given by the Pythagorean sum of $\Delta_{\rm BCS}$ and $\bar{\Delta}_{\rm ex}$, we found that the limit u in Eq. (14) is explicitly given by

$$u=\left\{(\hbar\omega_D)^2+\frac{\bar{\Delta}_{\rm ex}^2}{4}\exp\left[\frac{2}{JN_F^*}\right]\right\}^{1/2}\ . \tag{16}$$

Having found the limit u, the thermodynamic Eq. (14) can now be used to calculate the critical temperature T_c. Following the same procedure as in the BCS case and

evaluating the total gap Δ_T at $T=0$, we obtain

$$\Delta_T = 2u \exp\left[-\frac{1}{JN_F^*}\right], \tag{17}$$

where u is given by Eq. (16). Because of the presence of the phase factor Γ, the dimensionless factor in Eq. (16) has the following explicit form:

$$y \equiv JN_F^* = JN_F\{1/(1-X)^{1/2} - G^*[2\bar{\mu}(1-X)]\}^{1/2}, \tag{18}$$

where

$$X = (\Delta_{ex}/\bar{\mu})^2 . \tag{19}$$

By rearranging, we obtain

$$1-X = \frac{\gamma^4 W}{2y^4}, \tag{20}$$

where $\gamma = JN_F$ and

$$W = 1 - \frac{G^* y^2}{\bar{\mu}\gamma^2} + \left[1 - \frac{2G^* y^2}{\bar{\mu}\gamma^2}\right]^{1/2} . \tag{21}$$

As will be clear later, it is convenient to take y as a parameter in numerical analysis; the square of the total gap gives

$$\Delta_T^2 = 4u^2 \exp\left[\frac{-2}{y}\right] = (2\hbar\omega_D)^2 \exp\left[\frac{-2}{y}\right] + \frac{\bar{\mu}^2}{4}\left\{1 - \frac{\gamma^4}{2y^4} W\right\}^2 . \tag{22}$$

Following the BCS method, it is easy to show that the total gap is given in the weak coupling limit by

$$1 = JN_F^* \int_{-u}^{u} \frac{d\xi}{2\xi} \tanh\left[\frac{\xi}{2kT_c}\right] = JN_F^* \ln\frac{1.14u}{kT_c}$$

or

$$\Delta_T(0) = 1.75 kT_c . \tag{23}$$

Equating the right-hand sides of Eqs. (22) and (23), we have an algebraic equation involving the parameters T_c, y, $\bar{\mu}$, γ, and G^*:

$$(1.75kT_c)^2 = (2\hbar\omega_D)^2 e^{-2/y} + \frac{\bar{\mu}^2}{4}\left\{1 - \frac{\gamma^4}{2y^4} W\right\}^2 . \tag{24}$$

This is the crucial equation for the rest of our numerical analysis based on experimental data.[13] To simplify our analysis, we relate $\gamma = JN_F$ and $\bar{\mu}$ first because in the BCS theory[14–18] $\gamma = JN_F$ is taken to have the upper limit of 0.5 (Ref. 19) and $N_F \propto \sqrt{\varepsilon_F}$.

The experimental data provided by Bornemann and Morris[13] includes the result of the isotope-effect analysis with the undoped $YBa_2Cu_3O_7$ crystal. From electronic-band-calculated results,[20] we have learned that ε_F as measured from the valence-band (VB) maximum to the Fermi level is equal to 2 eV. Using as initial input $2\hbar\omega_D = 440$ K,[19] $\bar{\mu} = 2$ eV, $G^* \neq 0$, and $\gamma_0 = 0.46$, we obtain a unique solution for this undoped crystal: $\bar{\mu} = 2.0449$ eV, $G^* \cong 5\times10^{-7}$ eV, $\gamma = 0.4651$, $y = 0.4666$, and $\bar{\Delta}_{ex} = 0.013\,23$ eV, which indicate that the values of $\bar{\mu}$ and γ as given by band results are indeed quite accurate, except that in the band calculation G is approximately 1 eV.

It was found experimentally that a small structural change seems to have occurred during the superconducting transition, as reflected by the hardening of the ultrasound velocity.[21] Thus it is highly possible that the band gap G actually has collapsed in the superconducting state. Although the band gap G collapses, the semiconductinglike structure remains because the band gap is an indirect one in the Y-Ba-Cu-O system. We theorize that the structural change at T_c might be due to the internal electrostatic pressure of the condensed excitons. Using the approximate value that $\bar{\Delta}_{ex} \cong \Delta_{ex}^2/2\bar{\mu}$, we deduce $\Delta_{ex} \cong 0.2326$ eV. The band calculation also gives four intrinsic holes per unit cell within the VB,[20] and thus, summing over all the condensed positively charged excitons in the unit cell, we obtain an excitonic total binding energy in the unit cell of 4×0.2326 eV $=0.93$ eV, which is certainly close to the calculated band gap.[20] Hence, the collapse of the band gap during superconducting transition is predictable from the EEM theory.

To extend our analysis to La-doped data,[13] we must first ask what we might expect to change in the electronic structure caused by La doping of Ba. First of all, minor doping could be considered random, and its effect must also be described by a normal distribution. Second La

TABLE I. Parameters [χ—dopant, T_c—critical temperature, μ—chemical potential, J—BCS interaction, $N_f(0)$—density of states at Fermi level, $N_f^*(0)$—effective density of states at Fermi level, and G— band gap] best fitting the isotope substitution expermental data of Bornemann and Morris (Ref. 13).

χ	T_c (K)	μ (eV)	$JN_f(0)$	$JN_f^*(0)$	G (eV)
0.0	92.3	2.0449	0.4651	0.4666	5×10^{-7}
0.1	91.9	2.0604	0.4669	0.4684	5×10^{-7}
0.2	77.3	3.0237	0.5656	0.5665	5×10^{-7}
0.3	73	3.3525	0.5956	0.5963	5×10^{-7}
	60	3.3434	0.5948	0.5953	5×10^{-7}
0.4	49.3	2.9680	0.5604	0.5607	5×10^{-7}
0.5	38.3	2.3095	0.4943	0.4943	5×10^{-7}

TABLE II. Physical quantities (Δ_{ex}—excitonic gap, $\bar{\Delta}_{ex}$—effective excitonic gap, Δ_{BCS}—BCS gap, and Δ_T—total gap) calculated according to the EEM theory, using the sets of parameters in Table I.

χ	T_c (K)	Δ_{ex} (eV)	$\bar{\Delta}_{ex}$ (eV)	Δ_{BCS} (eV)	Δ_T (eV)
0.0	92.3	0.2326	0.013 23	0.004 448	0.013 95
0.1	91.9	0.2326	0.013 13	0.004 483	0.013 88
0.2	77.3	0.2420	0.009 686	0.006 489	0.011 66
0.3	73	0.2376	0.008 423	0.007 088	0.011 01
	60	0.1947	0.005 669	0.007 067	0.009 059
0.4	49.3	0.1510	0.003 839	0.006 372	0.007 439
0.5	38.3	0.1154	0.002 885	0.005 021	0.005 791

has a predominant valency of +3, while Ba has a predominant valency of +2; thus the doping of La should affect the density of carriers in the system. This effect could result in the change of the Fermi level, and thus $\bar{\mu}$. As $\bar{\mu}$ changes, so would the Fermi surface density N_F; thus both γ and y would also be affected. Accordingly, we use Eq. (24), by adjusting γ, and using $\bar{\mu}=2(\gamma/0.46)^2$ so as to obtain the T_c values given by the different dopant ratios χ. The results of our numerical analysis are shown in Tables I, II, and III. We can now plot the Fermi energy $\bar{\mu}$ versus dopant content χ in Fig. 1; the data are well fitted by

$$\bar{\mu}=D_1+D_2(\chi^2-D_3\chi)e^{-(\chi-D_4)^2/\sigma}, \tag{25}$$

where $D_1=2.044\,90$, $D_2=38.5801$, $D_3=0.080\,00$, $D_4=140\,00$, and $\sigma=0.200\,00$.

The term D_1 represents the undoped value of $\bar{\mu}$. The linear term in χ reflects an initial reduction in $\bar{\mu}$ due to uncorrelated distribution of La^{3+} ions in the crystal. Since each La provides three electrons to form the La^{3+} ion, while a Ba only provides two electrons to form a Ba^{2+} ion, the random presence of La in low quantities should reduce the intrinsic hole density. When the doping concentration of La is higher, these La ions would be strongly correlated to each other. The correlated effect on $\bar{\mu}$ is represented by the quadratic term in χ. Further, we plot $\bar{\mu}$ versus T_c in Fig. 2. The data points are found to fit a Fermi-Dirac distribution as follows:

$$\bar{\mu}=\frac{K_1T_c}{1+e^{K_2(T_c-T_3)}}, \tag{26}$$

where $K_1=0.062\,411\,1$, $K_2=0.0800\ \mathrm{K}^{-1}$, $T_3=85$ K. The Fermi-Dirac-like distribution implies a major effect of the presence of the dopant or $\bar{\mu}$ occurs at and around 85 K, and has a temperature spread of $K_2^{-1}=12.5$ K.

Likewise, we plot Δ_{BCS} versus T_c, and this is shown in Fig. 3. Again we obtain a fitting to the data by a Fermi-Dirac distribution.

$$\Delta_{BCS}=\frac{B_1T_c}{1+e^{K_2(T_c-T_3)}}, \tag{27}$$

where $B_1=0.000\,133\,6$.

K_2 and T_3 are found to be exactly the same as those given by the $\bar{\mu}$ distribution. Since the effect of doping on the forms of $\bar{\mu}$ is around T_3 in an exponential fashion as Δ_{BCS} is exponentially dependent on N_F^*, we expect that $\bar{\mu}$ and Δ_{BCS} have this exactly similar T_c dependency.

Now turning to the excitonic amplitude Δ_{ex} as a function of T_c. We note that Δ_{ex} is a function of the effective positive hole charge Z as given by the Bohr hydrogen ground state energy. A change of $\bar{\mu}$ would undoubtedly change Z, and thus T_c. Perhaps more important is the fact that dopant also relaxes the anisotropic conductivity property of the intrinsic holes. Thus dopant not only effects Z but it could also change the hydrogen binding from a two-dimensional (2D) character to the 3D characteristic. Since the ground-state energy of these two geometrical solutions differs by a factor of 4, we could expect the presence of dopant to reduce Δ_{BCS} significantly. If there is a finite band gap G in the normal state, the presence of sufficient dopant could actually break the excitonic condensation and thus also superconductivity itself according to the EEM theory. We plot Δ_{ex} versus T_c

TABLE III. T_c shift and isotope shift [α_0—isotope shift parameter (mass dependence of T_c): $T_c \propto 1/M^{\alpha_0}$] (theory cf. experiment).

χ	T_c	δT_c (calc.)	δT_c (expt.)	α_0 (calc.)	α_0 (expt.)
0.0	92.3	0.2905	0.29	0.026	0.025±0.002
0.1	91.9	0.4209	0.42	0.038	0.039±0.003
0.2	77.3	1.3308	1.33	0.143	0.140±0.003
0.3	73	1.7000	1.92	0.194	0.213±0.015
	60	1.9905	1.99	0.278	0.269±0.004
0.4	49.3	2.0201	2.02	0.337	0.324±0.013
0.5	38.3	1.5393	1.86	0.327	0.380±0.013

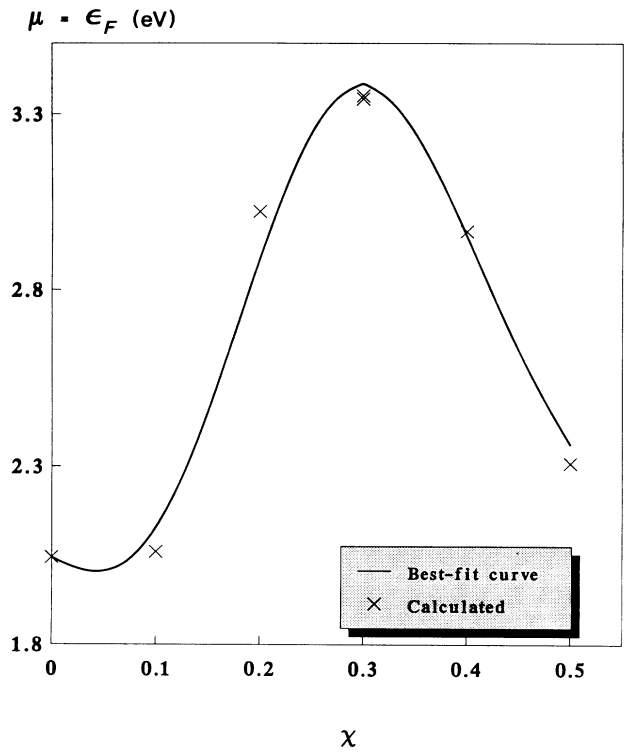

FIG. 1. Using certain data of Ref. 13, plots of the data points of the $\mu-\chi$ relation (χ measures the amount of dopant La). The solid line is described by expression (25).

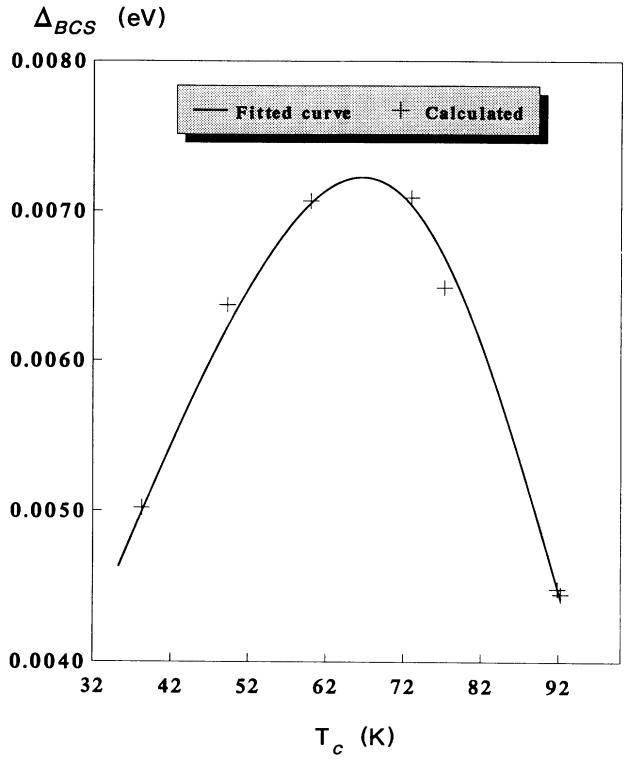

FIG. 3. Crosses demonstrating the calculated Δ_{BCS} (eV) vs $T_c(K)$ result. The solid line is expressed by relation (27).

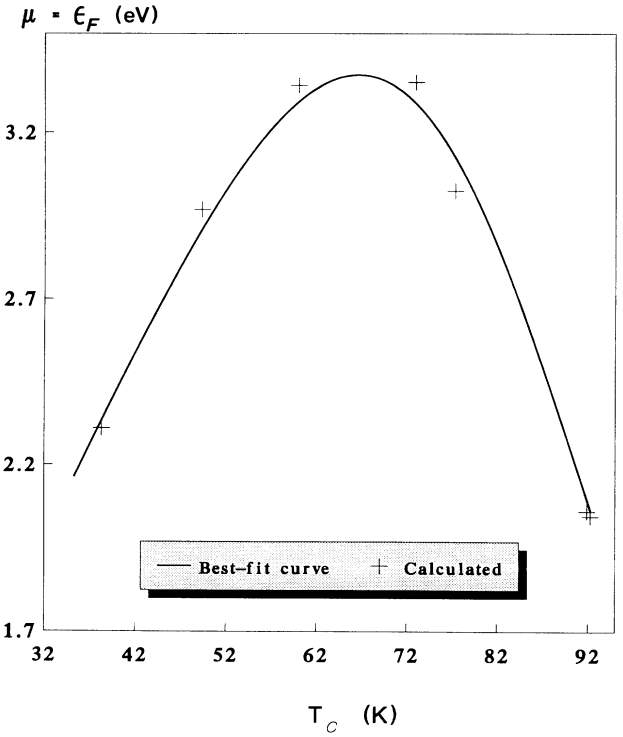

FIG. 2. The seven data points of the $\mu-T_c$ relation as deduced theoretically shown by crosses. The line of best fit can be described by the formula $\mu=K_1T_c/\{1+\exp[K_2(T_c-T_3)]\}$.

in Fig. 4. The data points can be fitted by a simple power law:

$$\Delta_{\mathrm{ex}}=A\left[1-\frac{T_1}{T_c}\right], \tag{28}$$

where $A=0.381$ eV and $T_1=30$ K.

In Ref. 13 the authors plotted the ionic mass power α_0 deduced from the isotope T shift data by assuming

$$T_c\propto\frac{1}{M^{\alpha_0}}. \tag{29}$$

With two isotope masses $M(\mathrm{O}_{16})$ and $M(\mathrm{O}_{18})$, we can readily show the α_0-T_c relation using

$$\ln[T_c(\mathrm{O}_{16})/T_c(\mathrm{O}_{18})]=\alpha_0\ln[M(\mathrm{O}_{18})/M(\mathrm{O}_{16})]\ . \tag{30}$$

Our theoretical result is indicated by the solid line in Fig. 5 and the experimental points of Ref. 13 are marked by dotted squares.

Finally, we wish to compare the theoretically deduced shift in critical temperature with that measured. In the first step, note that it is established already that in the BCS theory the BCS gap Δ_{BCS} suffers a shift if O_{18} replaces O_{16} according to a $M^{-1/2}$ relation. In other words, the change in Δ_{BCS} due to isotope substitution occurs in the change in ω_D alone as Δ_{BCS} is linearly proportional to ω_D. It is interesting to note that the line of best fit for the $\Delta_{\mathrm{BCS}}-T_c$ relation has the form specified by Eq. (27): The function $1/\{1+\exp[K_2(T_c-T_3)]\}$ has

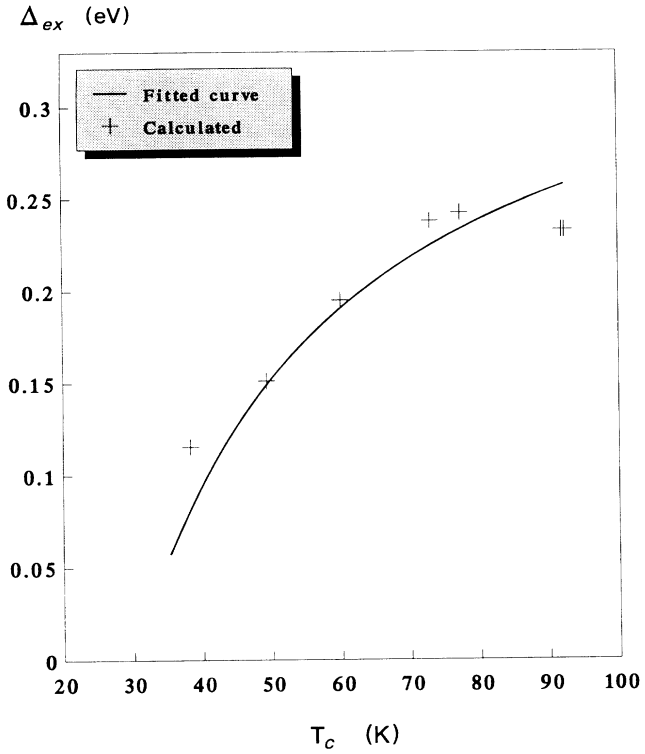

FIG. 4. The calculated excitonic gap parameter Δ_{ex} (in units of eV) corresponding to different T_c values indicated by crosses. The solid line is expressed by Eq. (28).

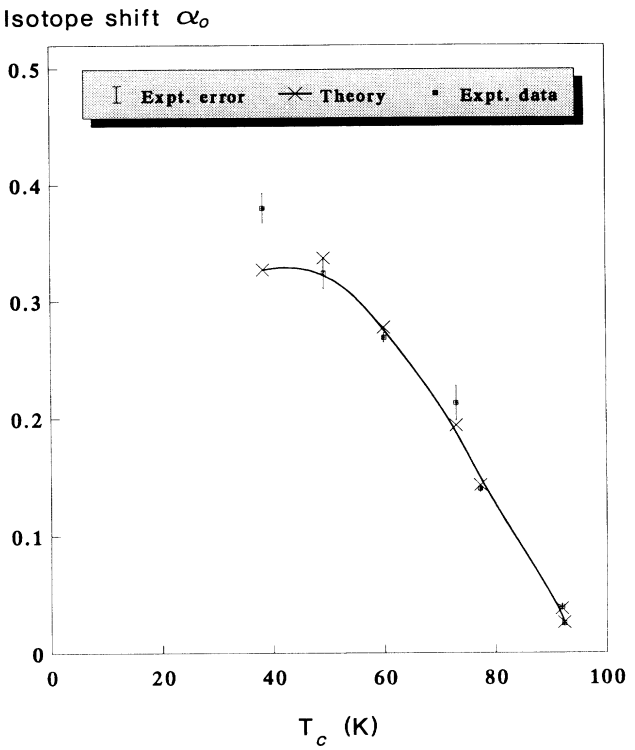

FIG. 5. Crosses representing the calculated isotope shift α_0 for different T_c values. The dotted squares with error bars are the experimental points in Ref. 13. The solid line is the line of best fit.

the same form as the Fermi-Dirac distribution and takes care of this type of statistics in the calculation of Δ_{BCS}, and the change in Δ_{BCS} due to the isotope effect, based on the argument just stated, can be taken to be

$$\delta\Delta_{\mathrm{BCS}}=\Delta_{\mathrm{BCS}}-\Delta_{\mathrm{BCS}}^{(i)}=\left\{1-\left[\frac{M(\mathrm{O}_{16})}{M(\mathrm{O}_{18})}\right]^{1/2}\right\}\Delta_{\mathrm{BCS}}(T_c)\ . \tag{31}$$

In review of relation (31), we can assume, at least correct to the lowest order approximation that δT_c and $\delta\Delta_{\mathrm{BCS}}$ are simply related by

$$\frac{\delta T_c}{T_c}=\frac{\delta\Delta_{\mathrm{BCS}}}{\Delta_T}\ . \tag{32}$$

As the isotope effect is only involved in Δ_{BCS} (rather than in $\bar{\Delta}_{\mathrm{ex}}$), in view of the Pythagorean relation, in the "no isotope" situation,

$$\Delta_{\mathrm{BCS}}^2+\bar{\Delta}_{\mathrm{ex}}\propto T_c^2\ , \tag{33}$$

and when O_{18} substitution has occurred,

$$\frac{M(\mathrm{O}_{16})}{M(\mathrm{O}_{18})}\Delta_{\mathrm{BCS}}^2+\bar{\Delta}_{\mathrm{ex}}^2\propto T_c^{(i)2}\ . \tag{34}$$

Then according to Eqs. (33) and (34), we readily find that

$$\frac{\delta T_c}{T_c}=\frac{(T_c-T_c^{(i)})}{T_c}$$
$$=1-\left\{\frac{[M(\mathrm{O}_{16})/M(\mathrm{O}_{18})]\Delta_{\mathrm{BCS}}^2+\bar{\Delta}_{\mathrm{ex}}^2}{\Delta_{\mathrm{BCS}}^2+\bar{\Delta}_{\mathrm{ex}}^2}\right\}^{1/2}\ . \tag{35}$$

Employing our numerical parameters K_1, K_2, T_3, etc., deduced from curve fitting, we can plot $\delta T_c/T_c$ (theory) against $\delta T_c/T$ (experiment). We observe that the points follow close to a straight line with slope $=45°$ (as shown in Fig. 6).

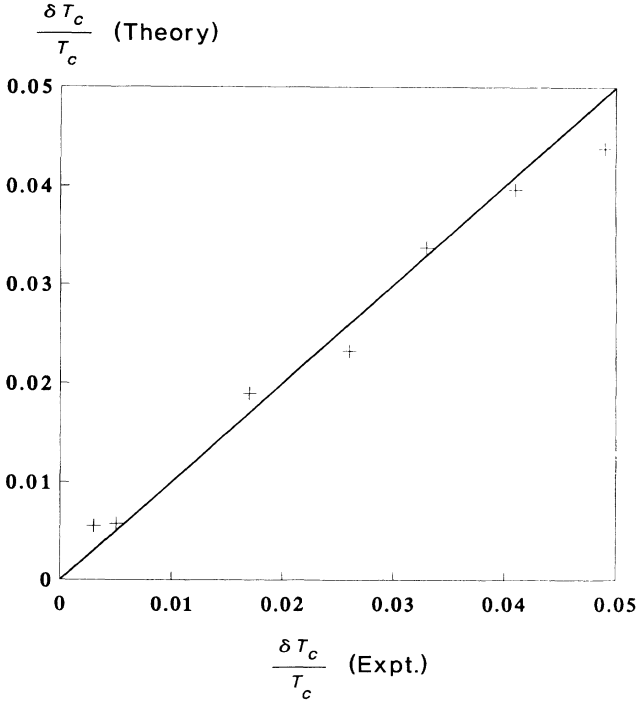

FIG. 6. $\delta T_c/T_c$ (theory) vs $\delta T_c/T_c$ (experiment).

IV. DISCUSSION

(1) A number of theories have been proposed (see, e.g., Refs. 22–29) to explain ceramic high-T_c superconductivity. With the advent of experimental results of various physical quantities, it is definitely a fruitful procedure to compare the consequences of any theory with observational data, in a detailed, quantitative manner. In particular, experimental isotope investigations offer quite accurate observational numbers of the shift of T_c and the "ionic mass power parameter α_0" according to relation (1). Previously, the range of α_0 and measurable δT_c cover rather narrow domains. Indeed, α_0 was found to lie within the range 0.0–0.02 for ceramic superconductors having $T_c \sim 90$ K. The recent report of Bornemann and Morris indicates that if we can dope the usual (123) specimen with La, the T_c and, hence, the α_0 values cover much wider ranges. We are therefore in a position to test the EEM theory by carrying out a detailed analysis of its consequence in relation to oxygen isotope substitution. Such an investigation would bring out certain key characteristics of the EEM.

(2) The essence of the EEM is the assumption of the existence of the condensation of charged excitons in the system. For different crystal structures of the ceramic high-T_c samples, it is highly likely that the Fermi level of the valence band could vary significantly. The lowest-energy level of the conduction band can also be varied significantly in these crystals so that the samples can be of the semimetallike type or semiconductorlike class. The value of the parameter G, a measure of the energy band gap between the valence and conduction bands, gives a very important hint to the electronic structure of the crystals. For example, if G is found to be very large, it would be highly unlikely for condensation of (quasiparticle) charged excitonic Cooper pairs to occur in the system. Another important feature of the EEM theory is that the total gap Δ_T (minimum energy between the ground and excited states of the electron or hole), is a Pythagorean sum of the effective excitonic excitation gap Δ_{ex} and that of the Δ_{BCS}. Physically, it means that Cooper pairs in the system are a mixture of holes and electrons. This analysis indicates that as the temperature rises, the quasiparticle Cooper pairs are gradually broken, releasing free holes and electrons until the sample loses superconductivity altogether and the free electrons drop back into the unfilled valence band. This features could lead to double discontinuities of the specific heat near T_c.[30]

(3) In the analysis of the experimental data,[13] we first utilize the band calculated parameters ε_F and γ (Ref. 20) for the perfect $YBa_2Cu_3O_7$ crystal. The relationship of T_c to $y \equiv \gamma\Gamma$ gives the unique solution $G^* \cong 0$ and the shift in T_c due to complete O_{18} substitution. The shift in T_c agrees precisely with the experimental value. Without a possible variation of T_c by doping with La and repeating the δT_c shift, the precise fitting of the calculated δT_c and that provided experimentally is of less significance because it is difficult to accurately compute the excitonic condensation gap Δ_{ex} from first principles so that no adjustable parameter is needed in the theory. The most difficult portion for carrying out a first-principles computation of Δ_{ex} is, in fact, due to the crystal anisotropy.[31,32] Our analysis of the experimental data for the wide range of the La-doped Y-Ba-Cu-O system, however, has to rely on fitting of ε_F and thus γ for each sample beyond simply Δ_{ex} is very satisfying because, first of all, these parameters ε_F, γ, and Δ_{ex} are mutually related to one another, but their variation relative to the undoped sample results are physically expected, and the variations are also within expected ranges. Finally the calculated results again give extremely close δT_c's to those measured experimentally (see Table III for details).

(4) It is also remarkable that the empirical formulas we obtained from the data fitting of $\bar{\mu}, \chi, T_c$ have physically meaningful forms as specified by Eqs. (25) and (26). As stated before, the denominators in Eqs. (26) and (27) are identical Fermi-Dirac distributions. Clearly, K_2T_2 represents $\Delta_T/(kT)$ in the terminology of quantum statistical mechanics, while K_2T_3 corresponds to the chemical potential divided by kT. The chemical potential and kinetic energy of the charged exciton pair are deduced, respectively, to be 85 K. Apart from the distribution function stated in Eq. (26), $\bar{\mu}$ also varies linearly with T_c. As the temperature is proportional to the kinetic energy, the $\bar{\mu} \propto T_c$ relation fits in the basic concept of physics. Following, expression (25) again seems to be consistent with intuition. D_1, of course, is the lower limit, a constant corresponding to the Fermi energy without La doping. The effect of doping certainly is described by the second term in Eq. (25). The moments of the Gaussian function $\exp[-(\chi - D_4)^2/\sigma^2]$ describe the random nature of the doping. So far, we cannot comment on the width σ and "peak" value D_4 based on doping by just one element, La. More sophisticated experimental doping results could lead us to a proper interpretation of the D_4 and σ values. It is also interesting to note that Δ_{ex} follows a power law with respect to T_c, and the index is -1 in this case. According to the EEM formulation, such a result is expected because of a change in carrier mass anisotropy.[31,32] The expression for Δ_{BCS} [see Eq. (27)] has the same form as that of $\bar{\mu}$, a result previously suggested from muon spin-relaxation experiments.[33]

(5) Because of a lack of other data, such as direct measurement of $\bar{\mu}$ on doping, we have to use experimental data points to obtain the lines of best fit for successive steps of analysis, arriving at empirical formulas (25)–(28). Future careful experiments to determine ε_F versus the amount of doping could give very important clues to the accuracy of EEM. Currently the agreement between theory and experimental results can be considered excellent, and the consequences of theoretical deduction seem to form self-consistent logic.

ACKNOWLEDGMENTS

The research of K.W.W. is partly supported by Midwest Superconductivity Inc. One of us (K.W.W.) thanks the Physics Department, University of Hong Kong for their hospitality while this work was completed.

*Permanent address: Department of Physics and Astronomy, University of Kansas, Lawrence, KS 66045.

[1]B. Batlogg, R. J. Cava, A. Jauaraman, R. B. van Dover, G. A. Kourouklis, S. Sunshine, D. W. Murphy, L. W. Rupp, H. S. Chen, A. White, K. T. Short, A. M. Mujsce, and E. A. Rietman, Phys. Rev. Lett. **58**, 2333 (1987); **60**, 754 (1988).

[2]L. C. Bourne, M. F. Crommie, A. Zettle, Hans-Conrad zur Loye, S. W. Keller, K. L. Leary, A. M. Stacy, and Don Morris, Phys. Rev. Lett. **58**, 2337 (1987).

[3]D. E. Morris, R. M. Kuroda, A. G. Markelz, J. H. Nickel, and J. Y. T. Wei, Phys. Rev. B **37**, 5936 (1988).

[4]E. L. Benitz, J. J. Lin, S. J. Poon, W. E. Farneth, M. K. Crawford, and E. M. McCaron, Phys. Rev. B **38**, 5025 (1988).

[5]S. Hoen, W. N. Creager, L. C. Bourne, M. F. Crommie, T. W. Barbee, M. L. Cohen, and A. Zettl, Phys. Rev. B **39**, 2269 (1989).

[6]L. C. Bourne, A. Zettl, T. W. Barbee, and M. L. Cohen, Phys. Rev. B **36**, 3990 (1987).

[7]C. Lin, Y. N. Wei, Q. W. Yan, G. H. Chen, Z. Zhang, T. G. Ning, Y. M. Ni, Q. S. Yang, C. X. Liu, T. S. Ning, J. K. Zhao, Y. Y. Shao, S. H. Han, and J. Y. Li, Solid State Commun. **65**, 869 (1988).

[8]B. Batlogg, G. Kourouklis, W. Weber, R. J. Cava, A. Jayaraman, A. E. White, K. T. Short, L. W. Rupp, and E. A. Rietman, Phys. Rev. Lett. **59**, 912 (1987).

[9]T. A. Faltens, W. K. Ham, S. W. Keller, K. J. Leary, J. N. Michaels, A. M. Stacy, H. C. zur Loye, D. E. Morris, T. W. Barbee, L. C. Bourne, M. L. Cohen, S. Hoen, and A. Zettl, Phys. Rev. Lett. **59**, 915 (1987).

[10]L. C. Bourne, S. Hoen, M. F. Crommie, W. N. Creager, A. Zettl, M. L. Cohen, L. Bernadex, J. Kinney, and D. E. Morris, Solid State Commun. **67**, 707 (1988).

[11]K. W. Wong and W. Y. Ching, Physica C **158**, 1 (1989).

[12]K. W. Wong and W. Y. Ching, Physica C **158**, 15 (1989).

[13]H. J. Bornemann and D. E. Morris, Phys. Rev. B **44**, 5322 (1991).

[14]D. Jerome, T. M. Rice, and W. Kohn, Phys. Rev. **158**, 462 (1967).

[15]J. Bardeen, L. N. Cooper, and J. R. Schrieffer, Phys. Rev. **108**, 1175 (1957).

[16]D. F. Lu, K. W. Wong, H. Y. Yeung, and P. C. W. Fung (unpublished).

[17]X. L. Yang, S. H. Guo, F. T. Chan, K. W. Wong, and W. Y. Ching, Phys. Rev. A **43**, 1186 (1991).

[18]S. H. Guo, X. L. Yang, F. T. Chen, K. W. Wong, and W. Y. Ching, Phys. Rev. A **43**, 1197 (1991).

[19]W. Weber and L. F. Mattheiss, Phys. Rev. B **37**, 599 (1988).

[20]W. Y. Ching *et al.*, Phys. Rev. Lett. **59**, 1333 (1987); G.-L. Zhao *et al.*, Phys. Rev. B **36**, 7203 (1987).

[21]D. J. Bishop *et al.*, Phys. Rev. B **35**, 8788 (1987).

[22]V. J. Emery, Phys. Rev. Lett. **58**, 2794 (1987).

[23]R. J. Birgeneau *et al.*, Z. Phys. B **71**, 57 (1988).

[24]P. W. Anderson *et al.*, Phys. Rev. Lett. **58**, 2790 (1987).

[25]H. Rietschel and L. J. Sham, Phys. Rev. B **28**, 5100 (1983).

[26]M. Grabowski and L. J. Sham, Phys. Rev. B **29**, 6132 (1984).

[27]C. N. Yang, Phys. Rev. Lett. **63**, 2144 (1989).

[28]J. E. Hirsch, Phys. Rev. Lett. **54**, 1317 (1985).

[29]W. Y. Kwok and P. C. W. Fung, J. Supercond. **3**, 395 (1990).

[30]S. E. Inderhees *et al.*, Phys. Rev. Lett. **60**, 1178 (1988); K. W. Wong and W. Y. Ching, Physica C **152**, 397 (1988).

[31]J. B. Torrance *et al.*, Phys. Rev. Lett. **60**, 542 (1988).

[32]I. Bozovic, J. Supercond. **4**, 193 (1991).

[33]Y. J. Uemura *et al.*, Phys. Rev. Lett. **62**, 2317 (1989).

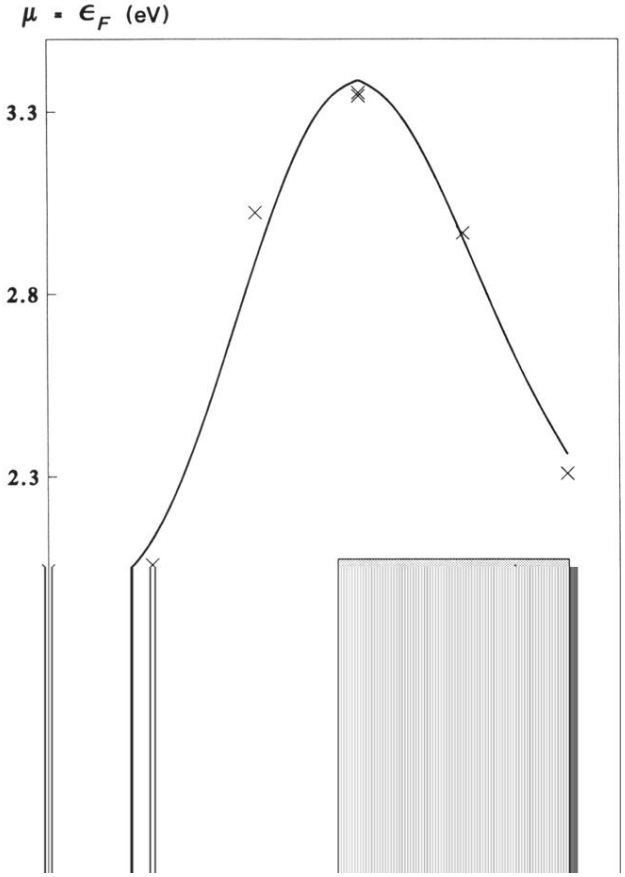
μ - ϵF (eV)
3.3
2.8
2.3

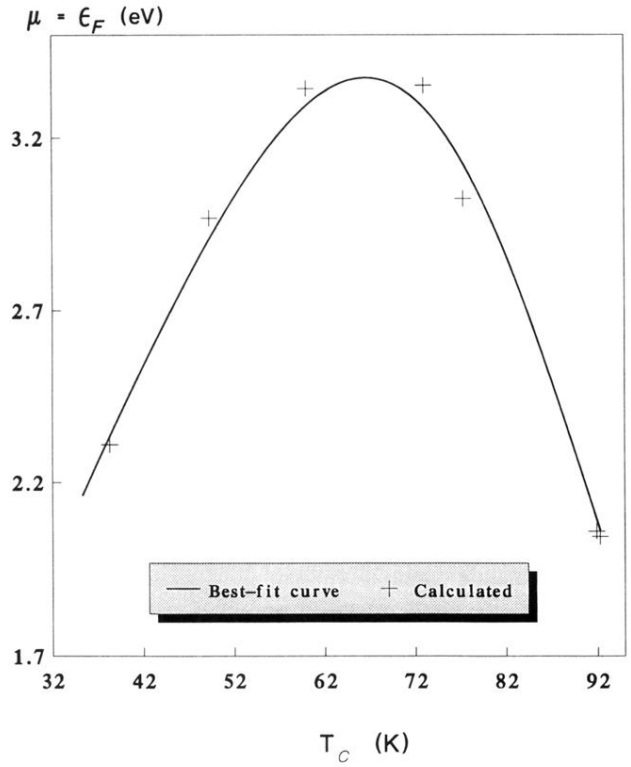

FIG. 2. The seven data points of the $\mu - T_c$ relation as deduced theoretically shown by crosses. The line of best fit can be described by the formula $\mu = K_1 T_c / \{1 + \exp[K_2(T_c - T_3)]\}$.

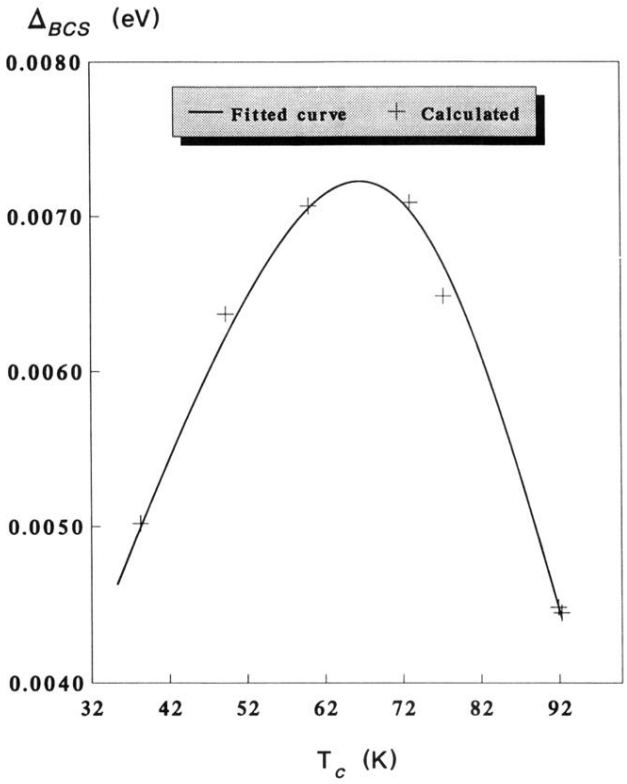

FIG. 3. Crosses demonstrating the calculated Δ_{BCS} (eV) vs $T_c(K)$ result. The solid line is expressed by relation (27).

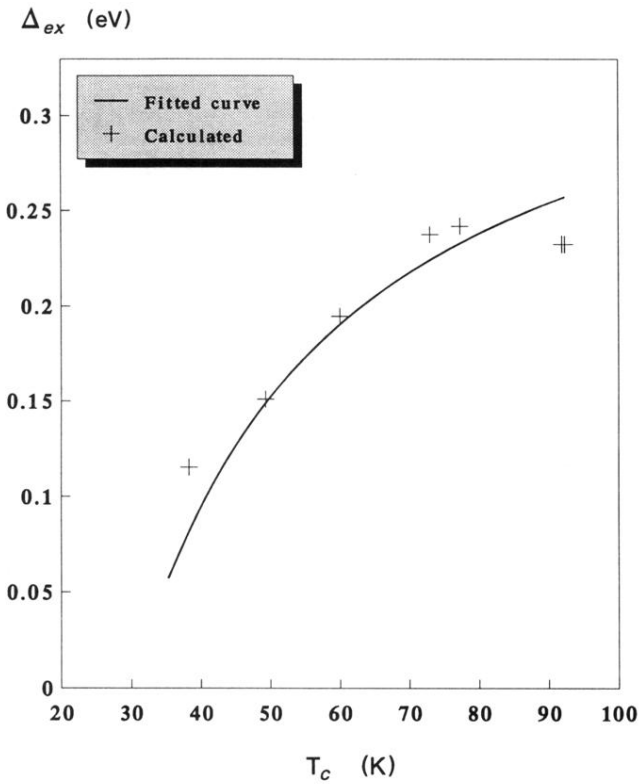

FIG. 4. The calculated excitonic gap parameter Δ_{ex} (in units of eV) corresponding to different T_c values indicated by crosses. The solid line is expressed by Eq. (28).

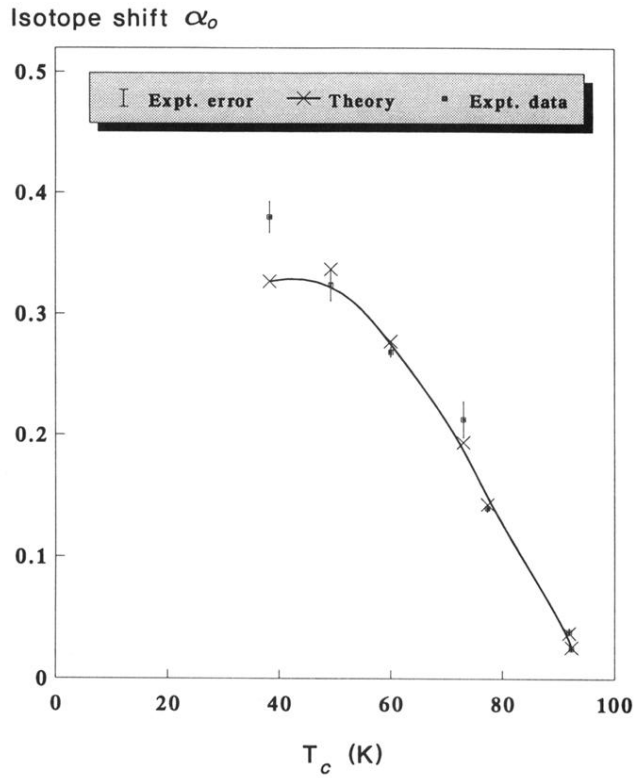

FIG. 5. Crosses representing the calculated isotope shift α_0 for different T_c values. The dotted squares with error bars are the experimental points in Ref. 13. The solid line is the line of best fit.